ELSEVIER

Contents lists available at ScienceDirect

# Journal of Inorganic Biochemistry

journal homepage: www.elsevier.com/locate/jinorgbio





# Kinetics of chromium(V)-oxo and chromium(IV)-oxo porphyrins: Reactivity and mechanism for sulfoxidation reactions

Tristan Skipworth, Mardan Khashimov, Iyanu Ojo, Rui Zhang

Department of Chemistry, Western Kentucky University, 1906 College Heights Blvd #11079, Bowling Green, KY 42101-1079, United States of America

#### ARTICLE INFO

Keywords: Chromium-oxo Porphyrin Sulfoxidation Thioanisole Kinetics Mechanism

#### ABSTRACT

In this work, chromium(IV)-oxo porphyrins [Cr<sup>IV</sup>(Por)(O)] (2) (Por = porphyrin) were produced either by oxidation of  $[Cr^{III}(Por)Cl]$  (1) with iodobenzene diacetate or visible light photolysis of porphyrin-chromium(III) chlorates. Subsequent oxidation of 2 with silver perchlorate gave chromium(V)-oxo porphyrins [CrV(Por)(O)] (ClO<sub>4</sub>) (3) in three porphyrin ligands, including 5,10,15,20-tetramesitylporphyrin(TMP, a), 5,10,15,20-tetrakis (2,6-difluorophenyl)porphyrin(TDFPP, b), and 5,10,15,20-tetrakis(pentafluorophenyl)porphyrin (TPFPP, c). Complexes 2 and 3 reacted with thioanisoles to produce the corresponding sulfoxides, and their kinetics of sulfoxidation reactions with a series of aryl methyl sulfides(thioanisoles) were studied in organic solutions. Chromium(V)-oxo porphyrins are several orders of magnitudes more reactive than chromium(IV)-oxo species, and representative second-order rate constants ( $k_{\rm ox}$ ) for the oxidation of thioansole are (0.40  $\pm$  0.01) M<sup>-1</sup> s<sup>-1</sup> (3a), and  $(2.82 \pm 0.20) \times 10^2 \,\mathrm{M}^{-1} \,\mathrm{s}^{-1}$  (3b), and  $(2.20 \pm 0.01) \times 10^3 \,\mathrm{M}^{-1} \,\mathrm{s}^{-1}$  (3c). The order of reactivity for 2 and 3 follows TPFPP > TDFPP > TMP, in agreement with the electrophilic nature of metal-oxo complexes. Hammett analyses indicate significant charge transfer in the transition states for oxidation of para-substituted thioanisoles by  $[Cr^{V}(Por)(O)]^{+}$ . The  $\rho^{+}$  constants are -1.69 for **3a**, -2.63 for **3b**, and -2.89 for **3c**, respectively, mirror values found previously for related metal-oxo species. A mechanism involving the electrophilic attack of the Cr<sup>V</sup>-oxo at sulfides to form a sulfur cation intermediate in the rate-determining step is suggested. Competition studies with chromium(III) porphyrin chloride and PhI(OAc)2 gave relative rate constants for oxidations of competing thioanisoles that closely match ratios of absolute rate constants from chromium(V)-oxo species, which are true oxidants under catalytic conditions.

#### 1. Introduction

Catalytic oxidation is one of the most critical processes conducted daily on a large scale for producing valuable chemicals and energy and the remediation of pollutants. [1–4] In nature, the superfamily of cytochrome P-450 enzymes (P450s) with a heme core catalyzes a wide variety of aerobic oxidations under mild conditions with exceptionally high reactivity and selectivity. [5,6] In the pursuit of controllable and efficient oxidation catalysis, many synthetic metal complexes such as metalloporphyrins have been largely synthesized as biomimetic catalysts for various catalytic transformations. [7–11] In enzymatic and synthetic oxidation catalysis, high-valent transition metal-oxo intermediates have been established as the active oxygen atom transfer

(OAT) species. [12–17] The direct detection and characterization of OAT metal-oxo species have provided a valuable rationale for oxidation processes. For example, iron(IV)-oxo porphyrin radical cations, termed compound I, have been extensively characterized as the active OAT species involved in the cytochrome P450 enzymes. [18] [19]

We have initiated a systematic study to elucidate the oxidation mechanism with a focus on the reactivity of the important high-valent metal-oxo intermediates. In this regard, we have employed chemical and photochemical methods to produce metal-oxo species supported by different macrocyclic ligands. [20] Thus, a number of high-valent metal-oxo intermediates, including Mn<sup>IV</sup>-oxo porphyrins, [21,22] Fe<sup>IV</sup>-oxo porphyrin radical cations and Fe<sup>IV</sup>-oxo neutral porphyrins, [23,24], *trans*-dioxo-Ru<sup>VI</sup>-porphyrins, [25,26] Mn<sup>V</sup>-oxo corroles, [27,28], Cr<sup>V</sup>-

Abbreviations: Por, porphyrin; TMP, 5,10,15,20-tetramesityphenylporphyrin; TDFPP, 5,10,15,20-tetrakis(2,6-difluorophenyl)porphyrin; TPFPP, 5,10,15,20-tetrakis(pentafluorophenyl)porphyrin; PhI(OAc)<sub>2</sub>, iodobenzene diacetate; PhIO, Iodosylbenzene; mCPBA, Meta-chloroperoxybenzoic acid; OAT, oxygen atom transfer; Salen, N,N-bis(salicylidine)ethylenediaminato).

E-mail address: rui.zhang@wku.edu (R. Zhang).

<sup>\*</sup> Corresponding author.

oxo salens, [29] and putative  $Fe^V$ -oxo corroles [30–32] and  $Ru^V$ -oxo porphyrins, [33,34] have been successfully generated and studied in real time. Upon forming these reactive metal-oxo transients, the kinetics of their oxidation reactions under easily established pseudo-first-order conditions have provided mechanistic insights into the identities of the active oxidants and oxidation reaction pathways of important catalysts. [20,35,36]

The chemistry of high-valent chromium-oxo porphyrins has received considerable attention as models of heme-containing enzymes, given their easy accessibility and stability. [37,38] In chromium porphyrin systems, two different high-valent chromium-oxo porphyrin species, i. e., chromium(V)- and chromium(IV)-oxo porphyrins, have been reported. [39-42] In contrast to extensive studies carried out on alkene epoxidations, [43-45] little is known with regard to reactivities and mechanisms of chromium(V)-oxo and chromium(IV)-oxo porphyrins in the sulfide oxidations. In this work, we report generation and kinetic studies of chromium(IV)- and chromium(V)-oxo porphyrins for the oxidation of thioanisoles in organic solutions. Notably, our kinetic results along with Hammett correlation and competition studies provide a unique opportunity to probe the sulfoxidation mechanism and catalytic roles of these metal-oxo species. To our knowledge, this study reports the first direct reactivity comparison and mechanistic analysis of Cr<sup>V</sup>and Cr<sup>IV</sup>-oxo porphyrins in the oxidation of thioanisoles under identical reaction conditions.

#### 2. Experimental

#### 2.1. Materials

All commercial reagents were analytic grades and used as supplied unless otherwise specified. Acetonitrile was obtained from Sigma Aldrich (HPLC grade) and passed through a dry alumina column before use. All organic substrates for kinetic studies were also purified by passing through a flash chromatography column of active alumina (Grade I) before use.  $\rm H_2^{18}O$  (97%  $^{18}O$ -enriched) was obtained from Sigma Aldrich. The pyrrole for porphyrin synthesis was freshly distilled before use. 5,10,15,20-Tetramesitylporphyrin,  $\rm H_2(TMP)(a)$ , 5,10,15,20-tetrakis(2,6-difluororophenyl)porphyrin,  $\rm H_2(TDFPP)(b)$ , and 5,10,15,20-tetrakis(pentafluorophenyl)porphyrin,  $\rm [H_2(TPFPP)](a)$ , were prepared according to known methods. [46] All chromium(III) chloride complexes [ $\rm Cr^{III}(Por)Cl$ ] (1a-c;  $\rm Por = porphyrin$ ) used in this work were prepared by the literature-reported method [47] and characterized by UV–vis and Infrared (IR).

#### 2.2. Instrumentation

UV-vis spectra were performed on an Agilent 8454 diode array spectrometer using standard 1.0-cm quartz cuvettes. Fast kinetic measurements were conducted on a stopped-flowed mixing spectrometer (Applied Photophysics SX-20). <sup>1</sup>H NMR (Nuclear Magnetic Resonance) was performed on a JEOL ECA-500 MHz spectrometer at 298 K with tetramethylsilane (TMS) as the internal standard. IR spectra were obtained on a Perkin Elmer FT-IR UATR spectrometer. Gas chromatography-mass spectrometry (GC-MS) analysis was performed on an Agilent GC7820A/MS5977B, coupled with an auto sample injector using an Agilent HB-5 capillary columns. Electrospray ionization-mass spectroscopy (ESI-MS) data were collected using an Agilent 500 LC-MS Ion Trap System. Visible light was produced from a SOLA SE II light engine (Lumencor) configured with a liquid light guide (6–120 W).

# 2.3. Generation of chromium(IV)-oxo porphyrins

Two methods were followed to generate the chromium(IV)-oxo porphyrins (2) in three porphyrin systems. In the first one, an excess amount of PhI(OAc)<sub>2</sub> (5 equiv.) was added to a  $CH_2Cl_2$  or  $CH_3CN$  solution of  $[Cr^{III}(Por)Cl]$  (1) in the range of concentrations from  $10^{-5}$  to

 $10^{-3}$  M at room temperature. The resulting mixture was stirred for 3–5 min to give the neutral [Cr<sup>IV</sup>(Por)O] products (2). The generated [Cr<sup>IV</sup>(Por)(O)] (2a-c) are stable in solution for days and can be further purified by flash column chromatography and characterized by <sup>1</sup>H NMR and IR, matching those reported. [48] Following our previous work, [20] the same [Cr<sup>IV</sup>(Por)(O)] (2a-c) were also photochemically generated by visible light irradiation of the photo-labile precursors [Cr<sup>III</sup>(Por) (ClO<sub>3</sub>)] (ca.  $1.0 \times 10^{-5}$  M) that was in-situ prepared by the facile axial ligand exchange of [Cr<sup>III</sup>(Por)Cl] (1) with excess AgClO<sub>3</sub>. The photochemical reactions became very slow or inert at higher concentration of the precursor (> $10^{-4}$  M), apparently due to light blocking. The UV–vis absorption spectra exhibited the same characteristic features for chromium(IV)-oxo porphyrins as observed in chemical oxidation methods. In both cases, the ESI-MS showed two prominent species, assigned to ion [(Por)Cr<sup>III</sup>]<sup>+</sup>, and ion [Cr(Por)(O)]<sup>+</sup>, respectively.

# 2.4. Generation of chromium(V)-oxo porphyrins

According to the literature-reported procedure, [42] one-electron oxidation of the chromium(IV)-oxo porphyrins with silver perchlorate leads to the formation of chromium(V)-oxo porphyrin perchlorates (3), i.e.  $[Cr^V(Por)(O)](ClO_4)$ . As described above, the chromium(IV)-oxo complexes (2) were first prepared in  $CH_2Cl_2$  with  $PhI(OAc)_2$ . Solid silver perchlorate (15 equiv.) was added, and the mixture was then stirred for 30 min. The excess silver perchlorate and silver chloride resulted from the reactions were filtered off, and the formation of the chromium (V)-oxo porphyrins was confirmed by their well-known UV-vis absorption spectra and ESI-MS. Due to their instability, complexes 3 were not further isolated and purified by column chromatography.

# 2.5. General procedure for preparative sulfoxidation reactions

Reactions for product analysis were carried out at a higher concentration of  $[\text{Cr}^{\text{IV}}(\text{Por})(\text{O})]$  or  $[\text{Cr}^{\text{V}}(\text{Por})(\text{O})]^+$  ( $\sim 10^{-4}$  M) and a large excess of thioanisole (same molar ratio range as kinetic studies) in 1 mL GC vial and monitored by UV–vis spectroscopy for completion of the reaction. Product yields were determined by GC analysis of the spent reaction solutions with an internal standards (1,2,4-trichlorobenzene), similar to our previously reported works. [22,49]

#### 2.6. Kinetic studies of chromium(IV)- and chromium(V)- oxo porphyrins

Reactions of chromium(IV) oxo-species **2** with an excess of organic sulfides (>100 equiv.) were conducted in an organic solution at  $23\pm 2\,^\circ \text{C}$ , monitored by UV–vis spectrometry. The rates of the reactions, which represented the rates of oxo group transfer from [Cr^IV(Por)O] to sulfides, were monitored by the decay of the Soret absorption band of **2**. The kinetic traces at  $\lambda_{\text{max}}$  of Soret band of [Cr^IV(Por)(O)] displayed good pseudo-first-order behavior for at least four half-lives, and the data was solved to give pseudo-first-order observed rate constants,  $k_{\text{obs}}$ . Plots of these values against the substrate concentration were linear in all cases. The second-order rate constants for reactions of the oxo species with the organic sulfides were solved according to Eq. (1). All second-order rate constants are averages of 2–3 determinations consisting of 4 independent kinetic measurements. Errors in the rate constants were weighted and are at  $2\sigma$ .

$$k_{\text{obs}} = k_0 + k_{\text{ox}}[\text{Sub}] \tag{1}$$

Sulfoxidation kinetics of chromium(V)-oxo species **3** was conducted in  $CH_3CN$  solutions similar to that of chromium(IV)-oxo species, except that a stopped-flow unit (SX-20) was employed. The rates of the reactions were monitored by the decay of the Soret band at 406 to 408 nm of  $[Cr^V(Por)(O)]^+$ .

Ar 
$$OCCl_2$$

Ar  $OCCl_2$ 

Ar

Scheme 1. Generation of chromium(IV)-oxo and chromium(V)-oxo porphyrins.

#### 2.7. Catalytic competition studies

A CH $_3$ CN solution containing equal amounts of two substrates, e.g., thioanisole (0.25 mmol) and substituted thioanisoles (0.25 mmol), and chromium(III) porphyrin catalyst (1 µmol) was prepared (final volume = 2 mL). PhI(OAc) $_2$  (0.1 mmol) as the limiting reagent was added, and the mixture was stirred at ambient temperature (23  $\pm$  2  $^{\circ}$ C) in the presence of a small amount of H $_2$ O (5 µL) for ca. 20 min. Relative rate ratios for catalytic oxidations were determined by GC based on the amounts of sulfoxide products. In this work, all the catalytic sulfoxidation reactions proceeded with good yields (> 95%), mass balance (> 95%), and no significant sulfones (< 1%) were detected. The ratio of product formation should reasonably reflect the relative sulfide reactivity toward the chromium(III)-catalyzed oxidations.

#### 3. Results and discussion

# 3.1. Formation of $[Cr^{IV}(por)(O)]$ and $[Cr^{V}(por)(O)](ClO_4)$

In metal-oxo chemistry, the consensus is that the reactivities of metal-oxo complexes are directly related to the electronic demand of the ligands, generally with the electron-withdrawing complexes being more reactive in view of their electrophilic nature. [50,51] Thus, we studied chromium complexes of three porphyrins that encompass the typical range of reactivities of these intermediates, 5,10,15,20-tetramesityllporphyrin (TMP, a), 5,10,15,20-tetrakis(2,6-difluoro)porphyrin(TPFPP, b), and 5,10,15,20-tetrakis(pentafluorophenyl)porphyrin (TPFPP, c) (Scheme 1). All porphyrin ligands with *ortho* substituents on phenyl rings are sterically encumbered, therefore, preventing unwanted chromium(III)  $\mu$ -oxo dimer formation. [52]

Depending on the reaction conditions, oxidation of chromium(III) porphyrin complexes with terminal oxidants such as iodosylbenzene (PhIO) or *meta*-chloroperoxybenzoic acid (mCPBA) are reported to generate  $Cr^{IV}$ -oxo (2) and/or  $Cr^{V}$ -oxo porphyrin (3) intermediates. For

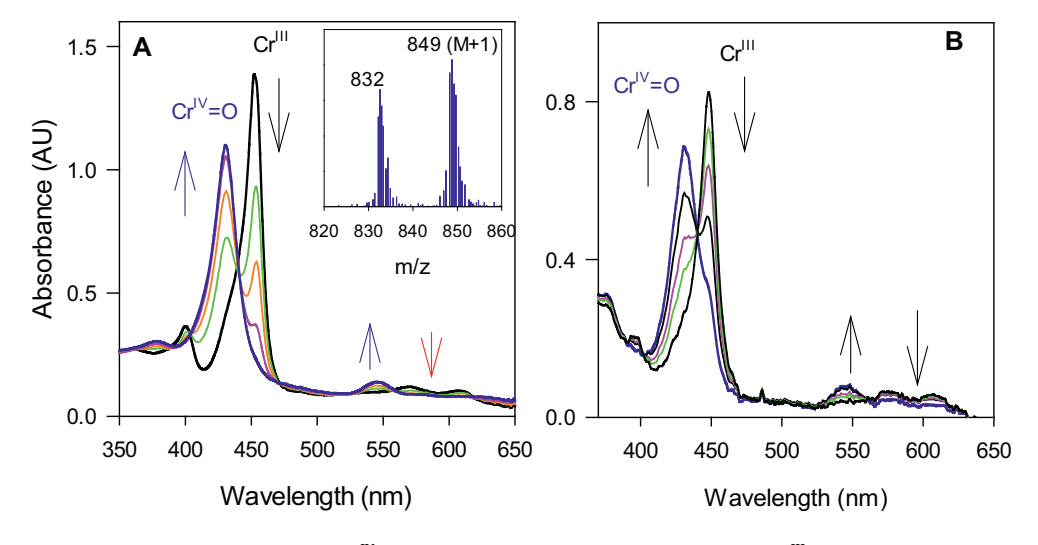


Fig. 1. (A) Time-resolved spectra showing the formation of  $[Cr^{IV}(TMP)(O)]$  (2a) in  $CH_2Cl_2$  by the oxidation of  $[Cr^{III}(TMP)Cl]$  (1a) with PhI(OAc)<sub>2</sub>, (5 equiv.) over 3 min. Inset is ESI-MS spectrum of 2a in a positive mode; (B) Photochemical formation of  $[Cr^{IV}(TMP)(O)]$  (2a) by visible light photolysis of  $[Cr^{III}(TMP)(ClO_3)]$  over 5 min.

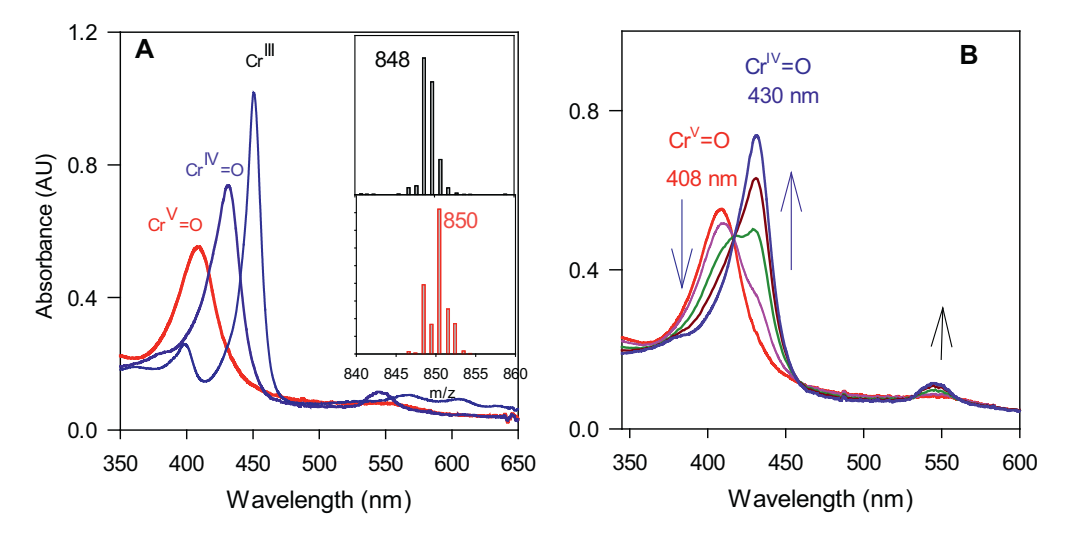


Fig. 2. (A) UV–vis spectra overlapped with  $[Cr^{II}(TMP)Cl]$  (black),  $[Cr^{IV}(TMP)(O)]$  (blue), and  $[Cr^{V}(TMP)(O)]^+$  (red); Insets showing the ESI-MS spectrum of  $^{16}O$ -labelled 3a (top) and  $^{18}O$ -labelled 3a (bottom); (B) Time-resolved spectra of the one-electron reduction of 3a with triethylamine (0.2 mM) in  $CH_3CN$  over 2 s. (For interpretation of the references to colour in this figure legend, the reader is referred to the web version of this article.)

example, treatment of  $[Cr^{III}(TMP)CI]$  with excess PhIO,  $[Cr^{V}(TMP)(O)]$  Cl was predominately produced (see Fig. S1 in Supplementary Material). In this study, chromium(IV)-oxo porphyrins (**2a-c**) in three different tetraarylporphyrin ligands were readily prepared using a mild oxygen donor PhI(OAc)<sub>2</sub> (Scheme 1). In contrast to PhIO which is insoluble in most organic solvents, PhI(OAc)<sub>2</sub> is readily soluble in organic media and safe to use. In many metal-catalyzed oxidation with PhI(OAc)<sub>2</sub>, a trace amount of water typically accelerates the oxidation rate because water could induce the steady-state formation of the more oxidizing PhIO from PhI(OAc)<sub>2</sub>, at the same time, release the stable HOAc instead of Ac<sub>2</sub>O under anhydrous conditions. [53,54]

As shown in titration experiment (see Fig. S2 in SI), 5 equivalents of PhI(OAc)<sub>2</sub> was needed to fully generate the chromium(IV)-oxo species. The oxidative transformation from  ${\bf 1a}$  to  ${\bf 2a}$  is characterized by a distinct UV-vis absorption change that showed a decay of the Soret band at  $\lambda_{max}$  451 nm peak of [Cr<sup>III</sup>(TMP)Cl] ( ${\bf 1a}$ ) and the formation of a blue-shifted Soret peak at 430 nm with Q-bands at 545 and 605 nm, matching characteristic absorption profiles of reported chromium(IV)-oxo porphyrins (Fig. 1A). The neutral  ${\bf 2a}$  was stable enough to be further purified and characterized by ESI-MS (positive mode), exhibiting a

prominent peak at a mass-to-charge ratio (m/z) of 849, matching the calculated M + 1 ion of [Cr(TMP)(O)]. Meanwhile, the diamagnetic nature of [Cr<sup>IV</sup>(TMP)(O)] was confirmed by obtaining the well-resolved <sup>1</sup>H NMR (see Fig. S3 in Supplementary Material). The more electrondemanding [Cr<sup>IV</sup>(TDFPP)(O)] (2b) and [Cr<sup>IV</sup>(TPFPP)(O)] (2c) were also formed in a similar fashion, and their spectra are in Supplementary Material (Fig. S4). The chemical generation of Cr<sup>IV</sup>-oxo porphyrins (2) can be ascribed to a possible comproportionation reaction that is well documented in the literature. [43,44] Because of the mild oxidizing nature of PhI(OAc)<sub>2</sub>, the chemical conversion of Cr<sup>III</sup> precursor (1) to initially formed CrV-oxo (3) was relatively slow; therefore, the concomitant comproportionation of CrV-oxo 3 with residual CrIII complex led to the thermodynamically favorable Cr<sup>IV</sup>-oxo species. Indeed, the formation of Cr<sup>IV</sup>-oxo species (2a) was observed when mixing Cr<sup>III</sup> complex (1a) with Cr<sup>V</sup>-oxo species (3a) that was independently prepared. [42]

Following our previous works, [20] the same [Cr<sup>IV</sup>(TMP)(O)] (2a) was also photochemically generated. Reaction of [Cr<sup>III</sup>(TMP)Cl] with excess AgClO<sub>3</sub> gave the photolabile chlorate complex [Cr<sup>III</sup>(TMP) (ClO<sub>3</sub>)], and a slightly blue-shifted Soret band (1–2 nm) in the UV–vis

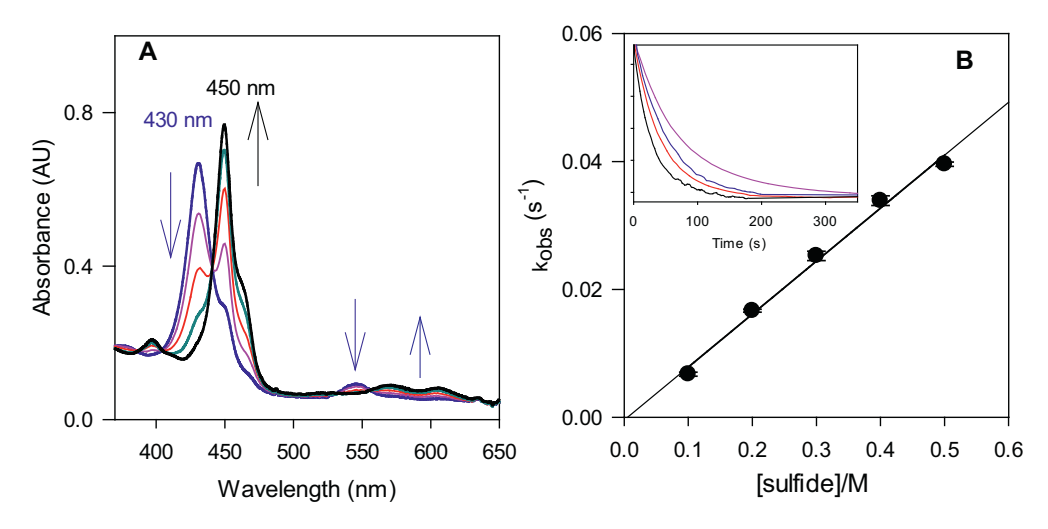


Fig. 3. (A) Time-resolved spectra of  $[Cr^{IV}(TMP)(O)]$  (2a) reacting in CH<sub>3</sub>CN solution with 4-fluorothioanisole(0.2 M) over 5 min at  $23 \pm 2$  °C; (B) Kinetic plot of the observed rate constants for the reaction of  $[Cr^{IV}(TMP)(O)]$  versus the concentrations of 4-fluorothioanisole. Inset showing traces at 430 nm for decaying of  $[Cr^{IV}(TMP)(O)]$  with different concentrations.

spectrum was found when the axial ligand is changed (see Fig. S5). Upon visible-light irradiation of  $[Cr^{III}(TMP)(ClO_3)]$  in  $CH_3CN$  or  $CH_2Cl_2$ ,  $[Cr^{IV}(TMP)(O)]$  was fully generated within 5 min, exhibiting the same UV–vis characteristic as that formed by chemical oxidation (Fig. 1 B). Accordingly, the photo-generation of  $[Cr^{IV}(TMP)(O)]$  is rationalized by homolytic cleavage of the O—Cl bond that resulted in one-electron oxidation. Similar one-electron photo-oxidation reactions were observed in our previous works on the generation of  $[Mn^{IV}(Por)(O)]$  [20] and  $[Mn^{V}(corrole)(O)]$ . [27] UV-light photolysis of the nitrito or nitrado chromium(III) tetraphenylporphyrin were previously reported by others to form the  $[Cr^{IV}(TPP)(O)]$  complex. [55,56] Under the same conditions, we found that photochemical cleavages of the chlorate complexes were considerably more efficient than cleavages of nitrito or nitrado complexes.

To generate higher valent chromium(V)-oxo species 3, we employed a one-electron oxidation approach according to the reported work. [42] As such, [Cr<sup>III</sup>(Por)Cl] was first oxidized by PhI(OAc)<sub>2</sub> (5 equiv.) to give [Cr<sup>IV</sup>(Por)(O)] species 2, which was subsequently oxidized by an excess amount of AgClO<sub>4</sub> in CH<sub>3</sub>CN (Scheme 1). The use of AgClO<sub>3</sub> or AgNO<sub>3</sub> as the one-electron oxidant instead of AgClO<sub>4</sub> gave similar results, albeit a longer time was required to complete the oxidation. The initially formed Cr<sup>V</sup>-oxo cation most likely coordinates with a perchlorate ion from the residual precursor instead of the solvent, since CH<sub>3</sub>CN was found to be too weakly binding solvent to replace the perchlorate ion in our previous studies. [35] Fig. 2A showed the representative absorption spectrum of [Cr<sup>V</sup>(TMP)(O)](ClO<sub>4</sub>) (3a) obtained by oxidation of the corresponding [Cr<sup>IV</sup>(TMP)(O)] (2a), the other two spectra for 3b and 3c are in Supplementary Material (see Fig. S6). Again, the ESI-MS measurement of 3a gave the molecular peak at m/z of 848 expected for  $[Cr(TMP)(^{16}O)]^{+}$ ion, which shifted to m/z of 850 in the presence of H<sub>2</sub><sup>18</sup>O upon <sup>18</sup>O isotope exchange (insets of Fig. 2A). To further validate the generation of CrV-oxo species, trimethylamine was used as a well-known oneelectron reductant, which rapidly reduced 3a to Cr<sup>IV</sup>-oxo (2a) species (Fig. 3B) and then less rapidly reduced 2a to Cr<sup>III</sup> complex (see Fig. S7 in Supplementary Material). The second-order rate constants for 3a and 2a reacting with the amine under pseudo-first order conditions were (2.25  $+ 0.28 \times 10^4$  and  $(2.20 + 0.10) \times 10^{-2} \,\mathrm{M}^{-1}.\mathrm{s}^{-1}$ , respectively.

#### 3.2. Sulfoxidation kinetics of chromium(IV)-oxo porphyrins (2)

Different from the chromium(V)-oxo species, all chromium(IV)-oxo porphyrins (2) generated in this study showed negligible reactivity toward alkenes and activated alkanes. In contrast, complexes 2 and 3 were found to be competent oxidants for sulfides. Product analysis of preparative reactions of both Cr<sup>IV</sup>-oxo (2a) and Cr<sup>V</sup>-oxo porphyrins (3a) with thioanisole showed the sulfoxide was only detected as the sole product in 76% and 95%, respectively, based on the oxo complexes used with a stochiometry of 1 mol oxo species producing 1 mol of sulfoxide. Negligible sulfone product from the over-oxidation of sulfoxide was detected (< 1% by GC). The representative GC analysis digram was shown in Supplementary Material (Fig. S8). Thus, oxidation kinetics of Cr<sup>IV</sup>-oxo species with a series of thioanisoles was first performed under pseudo-first-order conditions with solutions containing sulfide substrates (> 100 equiv.). The time-resolved spectra exhibited a clean conversion of Cr<sup>IV</sup>-oxo to Cr<sup>III</sup> product with isosbestic points in any of our studies (Fig. 3A). Similar to previously known oxidation of triphenylphosphine, [48] [Cr<sup>IV</sup>(Por)(O)] species could react with thioanisoles via a two-electron process to initially form CrII intermediate that subsequently follows a rapid aerobic oxidation to give the stable chromium (III) species as the final product. Attempt to detect the  $\mbox{Cr}^{\mbox{\scriptsize II}}$  intermediate under anaerobic conditions (degassed and protected by argon) was not successful, presumably due to its highly transient nature and/or residual oxygen sources such as PhI(OAc)<sub>2</sub> and AgClO<sub>3</sub>. For all Cr<sup>IV</sup>-oxo species, we monitored the decay of the Soret-band  $\lambda_{max}$  at 430 nm (2a), 426 nm (2b), and 420 nm (2c). Typical kinetic reaction profiles were shown for reactions of TMP oxo 2a in Fig. 3 and TDFPP oxo 2b, and TPFPP oxo 2c

Table 1
Second-order rate constants for chromium-oxo species 2 and 3.

Porphyrin	Substrate	[Cr <sup>IV</sup> (Por)O] ( <b>2</b> ) <sup>b</sup>	[Cr <sup>V</sup> (Por)O] <sup>+</sup> (3)	ratios <sup>c</sup>
TMP(a)	thioanisole	(3.00 ± 0.06)E-3	$0.40 \pm 0.01 (3.30 \pm 0.26)$ E-2 <sup>e</sup>	$\sim 10^2$
	4-fluorothioanisole	(8.40 ± 0.40)E-2	$0.33\pm0.08$	4
	4-chlorothioanisole	(6.64 ± 0.30)E-2	$0.13\pm0.01$	2
	4-methylthioanisole	$(8.87 \pm 0.50)$ E-2	$1.73\pm0.05$	19
	4- methoxylthioanisole	$(1.00 \pm 0.02)$ E-1	$5.80\pm0.06$	58
	cis-cycloctene	n.d. <sup>d</sup>	$(5.00 \pm 0.10)$ E-3	
	triethylamine	$(2.50 \pm 0.80)$ E-3	$(2.32 \pm 0.20)$ E3	~10 <sup>6</sup>
TDFPP ( <b>b</b> )	thioanisole	$\begin{array}{c} (1.18~\pm\\ 0.10)\text{E-2} \end{array}$	$(2.82 \pm 0.20)$ E2	~104
	4-fluorothioanisole	$(6.73 \pm 1.20)$ E-2	$(3.76 \pm 0.16)$ E2	~104
	4-chlorothioanisole		$(4.98 \pm 0.15)E1$	
	4-methylthioanisole		$(2.53 \pm 0.21)$ E3	
	4-		$(1.80 \pm 0.24)$ E4	
	methoxylthioanisole			
	cis-cyclooctene	n.d. <sup>d</sup>	$(3.8\pm0.2)\text{E-}2$	_
TPFPP (c)	thioanisole	$(1.40 \pm 0.20)$ E-2	$(2.20 \pm 0.10)$ E3	~10 <sup>5</sup>
	4-fluorothioanisole	$(4.36 \pm 0.80)$ E-1	$(2.52 \pm 0.66)$ E3	~10 <sup>4</sup>
	4-chlorothioanisole		$(1.21 \pm 0.10)$ E3	
	4-methylthioanisole		$(3.75 \pm 0.68)$ E4	
	4-		$(3.60 \pm 0.40)$ E5	
	methoxylthioanisole			
	cis-cyclooctene	n.d. <sup>d</sup>	$(8.01 \pm 0.20)$	

<sup>&</sup>lt;sup>a</sup> Second-order rate constant in CH<sub>3</sub>CN, unless specified, at 23  $\pm$  2 °C in units of M<sup>-1</sup> s<sup>-1</sup>. Reported values are the average of 2–3 runs with a deviation of 2 $\sigma$ .

<sup>b</sup> No appreciable different  $k_{\rm ox}$  obtained when the solvent is CH<sub>2</sub>Cl<sub>2</sub> instead of CH<sub>2</sub>CN.

in Supplementary Material (Figs. S9 and S10). The observed rate constants for the decay of **2** with sulfide substrates were fit reasonably well by pseudo-first-order solutions (Insets of Fig. 3B). The rate constants increased as a function of substrate concentration, and plots of  $k_{\rm obs}$  versus substrate concentration were linear (Fig. 3B). The second-order rate constants ( $k_{\rm ox}$ ) of sulfoxidation reactions with three Cr<sup>IV</sup>-oxo complexes (**2a-c**), as solved by Eq. (1), are so determined and collected in Table 1. Kinetic saturation of chromium-oxo species by sulfide substrates was not observed in all our studies. Of note,  $k_{\rm ox}$  values determined either by chemically or photochemically generated **2** were found to be in good agreement.

The second-order rate constants of [CrIV(Por)(O)] (2) obtained by this work demonstrated a relatively small kinetic effect of the porphyrin ligand and substrate. With thioanisole as the substrate, the values of  $k_{ox}$ are as follow: (3.00  $\pm$  0.06)  $\times$  10<sup>-3</sup> M<sup>-1</sup> s<sup>-1</sup> for **2a**, (1.18  $\pm$  0.10)  $\times$  $10^{-2} \, \mathrm{M}^{-1} \, \mathrm{s}^{-1}$  for **2b**, and  $(1.40 \pm 0.20) \times 10^{-2} \, \mathrm{M}^{-1} \, \mathrm{s}^{-1}$  for **2c**. In brief, the reactivity order of  ${f 2}$  with the same substrate follows TMP < TDFPP <TFPP, consistent with the expectation based on the electron demand of the porphyrin ligand. For a given oxo species, para-substituted thioanisoles react in a narrow kinetic range; the second-order rate constants for the oxidation of para-substituted thioanisoles with 2 are greater by less than one order of magnitude than that of thioanisole (Table 1). The kinetic data from the reaction of para-substituted thioanisoles permit Hammett analysis that showed non-linear correlations in all three systems, implying that no appreciable charge developed on the sulfur during the oxidation process by chromium(IV)-oxo porphyrins. Nonlinear Hammett plots have previously been observed for the reactions

<sup>&</sup>lt;sup>c</sup> Ratio of rate constants for **3** to **2**.

 $<sup>^{\</sup>rm d}$  Not detected due to no decay of species  ${\bf 2}$  in the presence of excess alkene substrate.

e In CH<sub>2</sub>Cl<sub>2</sub>.

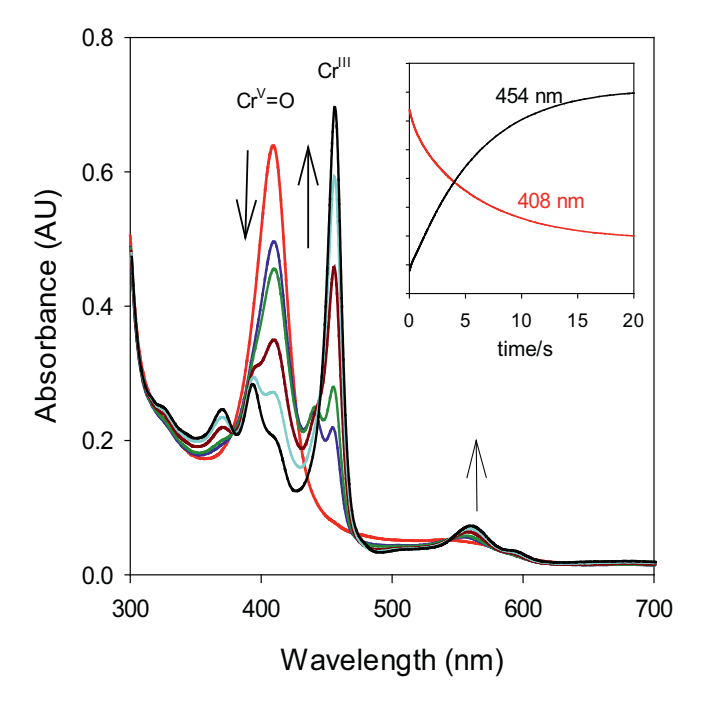


**Fig. 4.** Time-resolved spectrum for the decay of  $[Cr^V(TDFPP)(O)](ClO_4)$  (**3b**) in CH<sub>3</sub>CN containing 1 mM thioanisole over 20 s; the inset shows kinetic traces at 408 ( $Cr^V=O$ ) and 454 nm ( $Cr^{III}$ ) for the reaction.

of *para*-substituted thioanisoles, styrenes, and benzyl alcohols with iron (IV)-oxo porphyrins, which were ascribed to substantial development of radical character in the transition states. [49,57,58] In addition, we found that the rate constants of [Cr<sup>IV</sup>(Por)(O)] with sulfides in the polar solvent CH<sub>3</sub>CN are about as same as those in the less polar solvent CH<sub>2</sub>Cl<sub>2</sub>. This observation further implied that the transition state for the sulfoxidation reaction by **2** is not more polarized than the reactant ground state.

It is well-known in the literature that alkene epoxidation and benzylic C—H oxidations by the metal-oxo species could proceed via the rate-limiting formation of a radical intermediate. [2,59] Since the rate-limiting formation of a radical intermediate is usually associated with a moderate rate acceleration by both electron-donating and electron-withdrawing groups in the phenyl ring of the substrate [60,61] as

observed in the sulfoxidation of this study. Taken together, we propose that the reactions of chromium(IV)-oxo porphyrins with sulfides proceed through a mechanism involving the formation of radical intermediates from  $\text{Cr}^{\text{IV}}$ -oxo to sulfides. In such a radical pathway, its transition-state energy would be influenced by the polar substituent and spin delocalization effects since spin density develops at the sulfur atom upon progressing to the transition state.

#### 3.3. Sulfoxidation kinetics of chromium(V)-oxo porphyrins (3)

In a similar fashion to the kinetics of chromium(IV)-oxo porphyrins, the decay of chromium(V)-oxo species (3) in the presence of thioanisoles exhibited characteristic spectral changes with isosbestic points to regenerate the chromium(III) product. Compared to Cr<sup>IV</sup>-oxo 2, Cr<sup>V</sup>-oxo porphyrins (3) are much more reactive toward sulfides, reacting in <1 min in most cases. Therefore, a stopped-flow mixing unit was employed to conduct the kinetic measurements. Kinetics monitored the decay of the Soret band of chromium(V)-oxo species at 408 nm (3a), 406 nm (3b) or 406 nm (3c). A representative time-resolved spectra with kinetic traces for the sulfoxidation of [Cr<sup>V</sup>(TDFPP)O](ClO<sub>4</sub>) (3b) is shown in Fig. 4. Spectral examination of the spent reaction solutions showed that, with the low concentration of thioanisole (1 mM), only one [CrIII(TDFPP)] + product was formed (454 nm). With the higher concentration of thioanisole (4 mM), a mixture of [Cr<sup>III</sup>(TDFPP)]<sup>+</sup> and [Cr<sup>III</sup>(TDFPP)]<sup>+</sup>/thioanisole adduct was formed, showing a twin peak at 440 and 454 nm (see Fig. S11 in Supplementary Material). In a control experiment, we have found that the addition of a large excess of thioanisole (>1000 equiv.) shifted the Soret band of the [Cr<sup>III</sup>(TMP)](ClO<sub>4</sub>), not [Cr  $^{\mbox{\footnotesize III}}(\mbox{\footnotesize TMP})\mbox{\footnotesize Cl}],$  from 455 nm to 445 nm, suggesting that the sulfide could coordinate to the cationic chromium metal owing to the weakly binding nature of the perchlorate ion. Of note, the coordination process of sulfide to  $Cr^{III}$  ion also caused the disruption of the isosbestic point at 440 nm in the Fig. 4.

Previous studies of  $Cr^V$ -oxo porphyrins with less reactive alkenes have shown that the  $Cr^{IV}$ -oxo intermediate was concomitantly formed as a result of the competitive reaction of  $Cr^V$ -oxo and  $Cr^{III}$  product. [43,44] However, each of the sulfoxidation reactions with 3 studied in this work appeared to be a two-electron process with no formation of  $[Cr^{IV}(Por)O]$  (2). This spectral observation suggests that the rates of the reactions of  $Cr^V$ -oxo with the sulfides are faster than the competitive comproportionation of 3 with the formed  $Cr^{III}$  product due to their low concentrations ( $< 10^{-5}$  M). Again, each of the reactions of 3 with the substrates studied in this work showed first-order behavior with respect

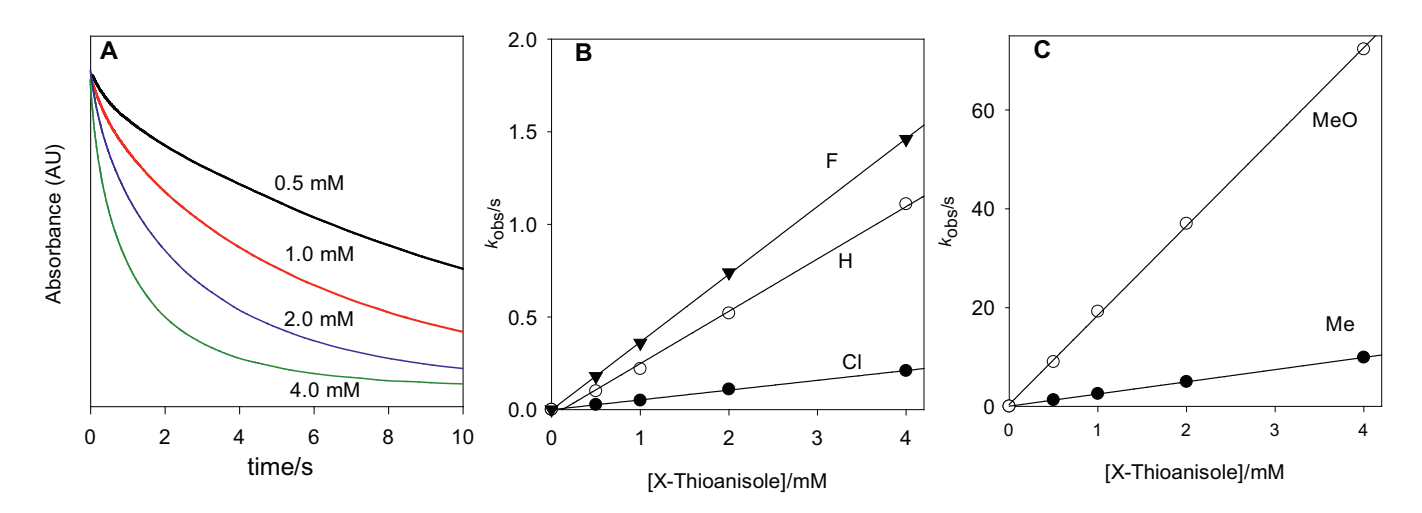


Fig. 5. (A) Kinetic traces at 407 nm (Soret band) for reactions of  $[Cr^{V}(TDFPP)(O)](ClO_4)$  (3b) with thioanisole (concentrations listed on the graph) in  $CH_3CN$ .; (5B—C) Observed pseudo-first-order rate constants for reactions of 3b in the presence of thioanisole and *para*-substituted thioanisoles (labels showing substituent on the *para*-position of thioanisoles).

to the substrate and first-order to the oxo species (Fig. 5 A). As shown in Figs. 5(B and C), the observed pseudo-first-order rate constants varied linearly with the concentration of substrates with near-zero intercepts, and the second rate constants from the slopes are summarized and compared with those of  $\bf 2$  in Table  $\bf 1$ .

For comparison, the oxidation of *cis*-cyclooctene by **3** in CH<sub>3</sub>CN under the same conditions showed similar kinetic profiles that occurred in the oxidation of thioanisoles. Noticeably, the rate constants for *cis*-cyclooctene oxidation ranged from  $(5.00\pm0.10)\times10^{-3}$  (**3a**),  $(3.80\pm0.20)\times10^{-2}$  (**3b**) to  $(8.01\pm0.20)$  (**3c**)  $M^{-1}$  s<sup>-1</sup>, which are about 3 to 5 orders of magnitude smaller than that for the oxidation of thioanisoles with the same Cr<sup>V</sup>-oxo species. Similarly, our prior studies with iron(IV)-oxo porphyrins [49] and manganese(V)-oxo corroles [27] showed that sulfoxidation reactions were 3 to 4 orders of magnitude faster than those oxidations of alkenes and activated C—H bonds by the same oxo species, primarily due to the enhanced nucleophilicity and easy access of sulfide versus hydrocarbons.

Little kinetic data existed for comparison to the rate constants for  $Cr^V$ -oxo complexes (3) determined in this work. Bruice and co-workers studied epoxidation reactions of alkenes with  $[Cr^V(TDCPP)(O)](ClO_4)$  (TDCPP = 5, 10, 15, 20-tetrakis-2,6-dichloroporphyrin) system in  $CH_2Cl_2$  solutions with a rate constant of  $2.13 \times 10^{-2} \ M^{-1} \ s^{-1}$  for epoxidation of *cis*-cyclooctene, [43] which appears to be consistent with our finding that  $[Cr^V(TDFPP)(O)](ClO_4)$  (3b) reacted with *cis*-cyclooctene in  $CH_3CN$  with a rate constant of  $(3.80 \pm 0.20) \times 10^{-2} \ M^{-1} \ s^{-1}$ . In comparison to 3a, a similar reactivity was observed in the sulfide oxidation by  $[Ru^{VI}(TMP)O_2]$  [62] and  $[Ru^{IV}(bpy)_2(O)PR_3](ClO_4)$  (bpy = 2,2'-bipyridine). [63]. The oxidation kinetics of substituted thiosnisole was studied by salen-manganese(V)-oxo [64] and salen-chromium(V)-oxo species, [65] whereas the rate constants in the range of  $10^{-3}$  to  $10^{-2} \ M^{-1} \ s^{-1}$  were several orders of magnitude smaller than those by  $Cr^V$ -oxo porphyrins obtained in this study.

# 3.4. Mechanistic consideration on sulfoxidation reactions by $[Cr^V(por)](O)$ [ClO4]

Inspection of the second-order rate constants in Table 1 revealed several interesting kinetic aspects of the chromium-oxo porphyrins. All thioanisoles were successfully oxidized by [CrIV(Por)(O)](2) and [Cr<sup>V</sup>(Por)(O)](ClO<sub>4</sub>)(3). Clearly, the higher valent chromium(V)-oxo species 3 are several orders of magnitude more reactive than the corresponding chromium(IV)-oxo **2**. Both [Cr<sup>IV</sup>(Por)(O)](**2**) and [Cr<sup>V</sup>(Por) (O)](ClO<sub>4</sub>)(3) with the same substrate follow the trends in reactivity of TPFPP>TDFPP>TMP, consistent with the expected increase in the electrophilicity of metal-oxo species. One of the more noteworthy aspects is that the kinetic effect derived from the porphyrin ligands in chromium(V)-oxo species 3 is substantial in comparison to [Cr<sup>IV</sup>(Por) (O)](2). For example, the second-order rate constants for oxidations of thioanisole by the chromium(V)-oxo **3a-c** are 0.4,  $2.8 \times 10^2$ , and  $2.2 \times 10^2$ 10<sup>3</sup> M<sup>-1</sup> s<sup>-1</sup>, respectively. The seemingly electron-deficient TDFPP and TPFPP systems displayed particularly accelerating kinetic effects, and ratios of reactivities of 3 versus 2 range from 4 to 5 orders of magnitude in TDFPP and TPFPP compared to only one order of magnitude in TMP (Table 1). Likewise, the rate constant for epoxidation of cis-cyclooctene by 3c (TPFPP) is 210 and 1600 times greater than the rate constants for the same oxidation by 3b (TDFPP) and 3a (TMP), respectively. In addition to the expected increase in the electrophilicity in the TDFPP and TPFPP systems, the significant ligand effect of chromium (V)-oxo species observed in sulfoxidation reactions might implicate a much more polarized transition state of oxidation processes. On top of that, a dramatic solvent effect on the sulfoxidation kinetics of CrV-oxo species has been noted (Table 1), and the rate of constant for sulfoxidation of thioansole by **3a** in CH<sub>3</sub>CN ( $k_{ox} = 0.4 \text{ M}^{-1} \text{ s}^{-1}$ ) was >10 times greater than that in the less polar solvent of CH<sub>2</sub>Cl<sub>2</sub> ( $k_{ox} = 3.30 \times 10^{-2} \text{ M}^{-1} \text{ s}^{-1}$ ). Apparently, increasing the polarity of solvent that gave rise to a faster reaction is consistent with expectations that charge is more localized in

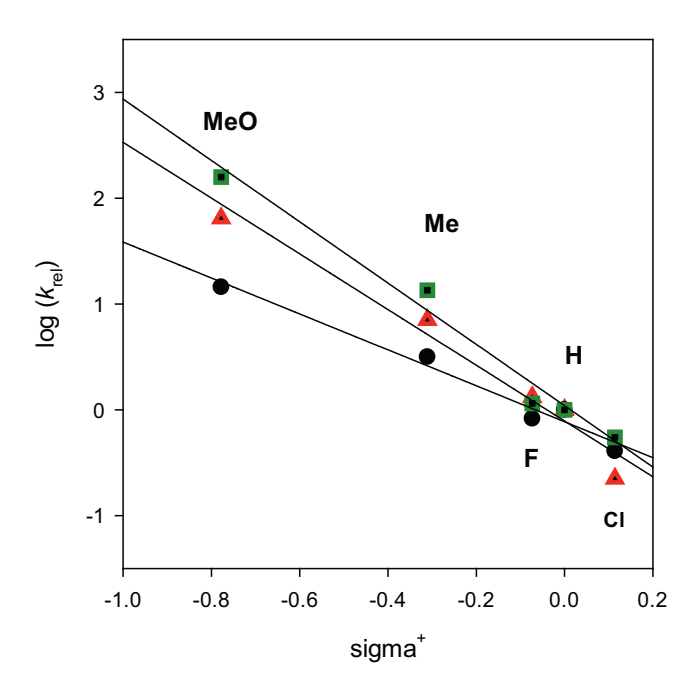


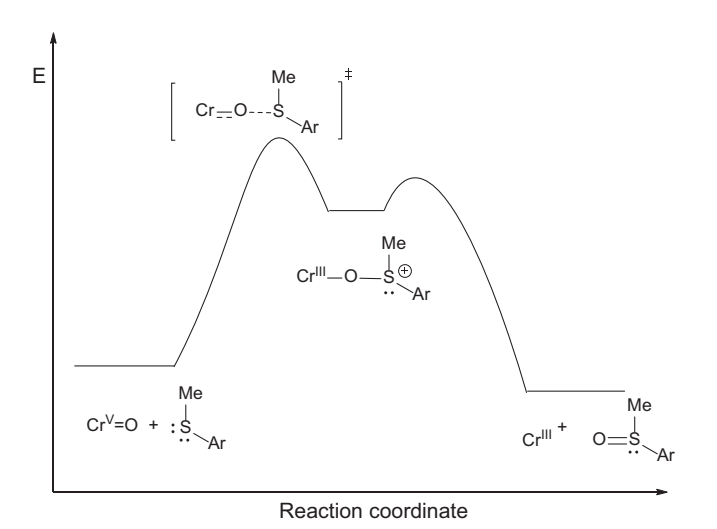
Fig. 6. Linear Hametten plots for reactions of *para*-substituted thioanisoles with  $Cr^V$ -oxo 3a (circle), 3b (triangle), and 3c (square), where the labels indicate the substituent on thioanisoles.

the transition states than in the reactants.

A further reflection of the electronic demands in the transition states of the oxidation reactions is seen in the oxidation of the para-substituted thioanisoles by 3. In all three systems studied here, we observed a clear substituent dependence on the second-order rate constants for the parasubstituted thioanisoles (Y-thioanisoles; Y = 4-MeO, 4-Me, 4-F, and 4-Cl). In particular, the electron-donating substituents (Me and MeO) in the para position of phenyl group of thioanisoles substentially increased the rate constants (Fig. 5B-C). Linear correlations ( $R \ge 0.97$ ) of logk- $_{\rm rel}[k_{\rm rel} = k(Y-thioanisole)/k(thioanisole)]$  versus Hammett  $\sigma^+$  substituent constants were obtained as shown in Fig. 6. The slopes  $(\rho^+)$  of plots are negative, ranging from  $-1.69 \pm 0.17$  for **3a**,  $-2.63 \pm 0.31$  for **3b**, to  $-2.89 \pm 0.29$  for **3c**, respectively, suggesting a significant positive charge developed on the sulfur center of the transition state in ratelimiting steps. Linear Hammett plots with similar  $\rho^+$  values were also found in the oxidations of para-substituted thioanisoles by [Mn<sup>V</sup>(salen) (O)]  $(\rho^+ = -1.85)$ , [64,66]  $[Cr^V(salen)(O)]$   $(\rho^+ = -2.7)$ , [65]  $[Ru^{IV}(b-1.85)]$ py)<sub>2</sub>(O)PR<sub>3</sub>] (bpy = 2,2'-bipyridine) ( $\rho^+$  = -1.56), [63] and [Mn<sup>V</sup>(TPFC)(O)] (TPFC = 5,10,15-tris-pentafluorophenylcorrole) ( $\rho^+$  =

Although the free energy relation of log  $k_{rel}$  versus  $\sigma^+$  does not uniquely define the reaction mechanism, it provides insights into the mechanism of sulfoxidation with  $Cr^V$ -oxo porphyrins. If we compare the reactivity of three  $Cr^V$ -oxo complexes with the  $\rho^+$  values that displayed a substantial difference based on the electron demand of the ligand, the concerted oxygen insertion, i.e.,  $S_N 2$  mechanism, can be excluded. If the direct oxygen transfer operates, an inverted trend of the reactivity-selectivity ( $\rho^+$  values) should be obtained, i.e., the most reactive 3c should give the smallest  $\rho^+$  values, [68] which is apparently opposed to the actual experimental results. Our spectral studies also ruled out the operation of the single electron-transfer(SET) mechanism that would have formed  $Cr^{IV}$ -oxo intermediate in the rate-determining step. As noted early, we have not observed any spectral evidence for the formation of  $Cr^{IV}$  species during the course of all sulfoxidation reactions.

On numerous occasions, a cationic intermediate has been proposed for the epoxidation of alkenes by high-valent metal-oxo porphyrins. [45,69,70] Since the free-energy relationship of log $k_{\rm rel}$  versus  $\sigma^+$  suggests a significant positive charge developed on the sulfur of the



**Scheme 2.** A proposed mechanism for sulfoxidation reactions by Cr<sup>V</sup>-oxo porphyrins.

transition state, it would appear possible that the sulfoxidation by  $Cr^V$ -oxo porphyrins can be characterized by the electrophilic attack of the oxidant at the sulfur atom that resulted in a sulfur cation intermediate in the rate-determining step, which is further supported by the observed solvent and porphyrin ligand effects. Moreover, a stepwise mechanism involving the sulfur cation intermediate was previously proposed in related sulfoxidation reactions by  $[Cr^V(salen)O]^+$  complexes with a similar  $\rho^+$  value ( $\rho^+=-2.7$ ). [65] Thus, the proposed mechanism in Scheme 2 provides the most logical rationalization of the experimental results in the present work. It is worthwhile to note that the reported  $\rho^+$  values (-3.6 to -4.8) [71,72] for those electrophilic additions to alkenes involving a carbocation in the rate-determining steps are greater than the  $\rho^+$  values (-1.7 to -2.8) determined in the present sulfoxidation, presumably due to the different level of charge transfer on cationic atoms (carbocation versus sulfurcation).

#### 3.5. Competition studies of catalytic sulfoxidations

One objective of our studies is to identify the kinetically competent oxidants during catalytic turnover conditions that could lead to a better understanding of the reaction mechanism. However, in most catalytic reactions the concentrations of active oxidants do not accumulate to detectable concentrations. Furthermore, our previous studies with various high-valent metal-oxo species indicate that a high-valent metaloxo species detected in a reaction might not be the true oxidant in the system. [20,36] In this regard, chromium porphyrin complexes have been used as synthetic catalysts for various oxidation reactions, where the involvement of high-valent metal-oxo species was indicated. [37,38,45] Similarly, we have found that chromium(III) porphyrins catalyzed efficient oxidation of sulfides in the presence of PhI(OAc)2. For example, under optimized conditions, i.e., 0.2 mol% of [CrIII(Por)Cl] (1), 0.5 mmol substrate and 0.75 mmol PhI(OAc)2 in 2 mL CH3CN containing 5 µL H<sub>2</sub>O at room temperature, thioanisole was quantatively oxidized to the corresponding sulfoxide product with 93% selectivity. Thus, we have attempted to determine whether the generated chromium-oxo species observed in our kinetic studies is the actual oxidant formed during catalytic conditions. To assess whether the same oxo species is active in the two sets of conditions, one can compare the ratios of products formed under catalytic turnover conditions to the ratios of absolute rate constants measured in the direct kinetic studies.

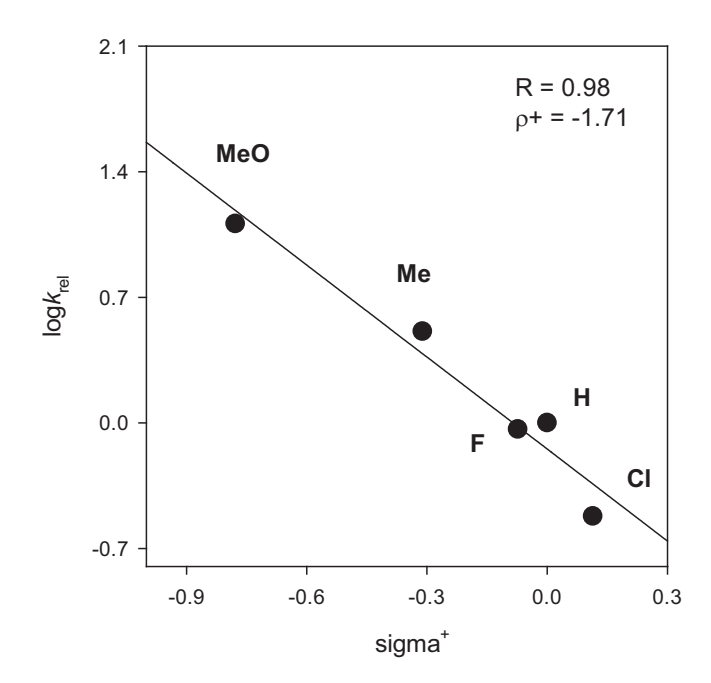
Toward this end, we carried out a set of competitive oxidations using  $[Cr^{III}(Por)Cl]$  (1) as catalysts with PhI(OAc)<sub>2</sub> as the oxygen source as described in the experimental section. In catalytic competition studies, a

Table 2
Relative rate constants from kinetic studies and competition catalytic oxidations <sup>a</sup>

Porphyrin	Substrates	Rate constant ratios by 2 <sup>b</sup>	Rate constant ratios by <b>3</b> <sup>c</sup>	PhI (OAc) <sub>2</sub> <sup>d</sup>
ТМР	<i>p</i> -F-PhSMe/ PhSMe	28	0.83	0.92
	<i>p</i> -Cl-PhSMe/ PhSMe	22	0.33	0.30
	<i>p</i> -Me-PhSMe/ PhSMe	30	4.0	3.2
	<i>p</i> -MeO-PhSMe/ PhSMe	33	14.0	13.0
TDFPP	<i>p</i> -F-PhSMe/ PhSMe	5.6	1.33	1.10
TPFPP	<i>p</i> -F-PhSMe/ PhSMe	3.1	1.15	1.01

 $<sup>^</sup>a$  A reaction solution containing equal amounts of two substrates, e.g., thio-anisole (0.25 mmol) and substituted thioanisole (0.25 mmol), chromium(III) porphyrin catalyst (1 µmol) was prepared in CH<sub>3</sub>CN (2 mL). Iodobenzene diacetate PhI(OAc) $_2$  (0.1 mmol) was added with 5 µL H $_2$ O, and the mixture was stirred for ca. 15 min at room temperature.

 $<sup>^{\</sup>rm d}$  Ratios of relative rate constant from competitive oxidations with chromium (III) porphyrin catalysts at ambient temperature. All competition ratios are averages of 2–3 determinations with  $\pm 5\%$ standard deviations of the reported values.

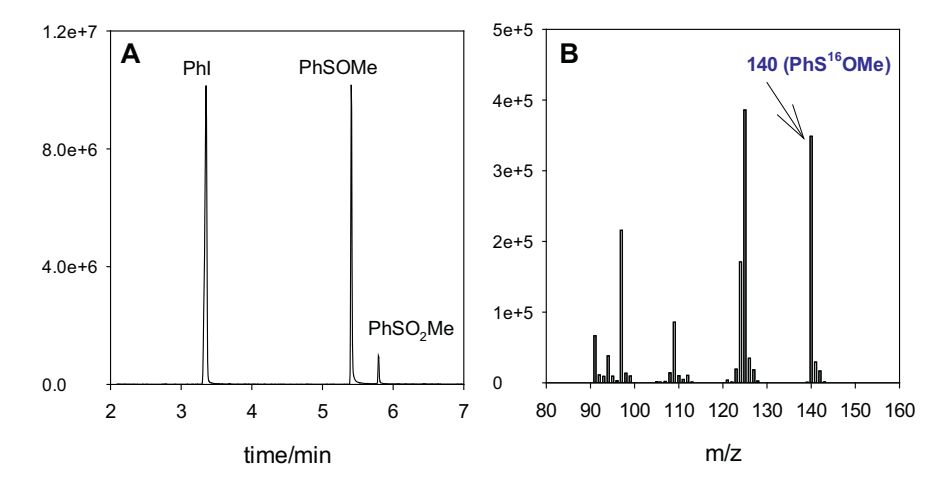


**Fig. 7.** Hammett correlation studies (log  $k_{rel}$  vs  $\sigma^+$ ) for the [Cr<sup>III</sup>(TMP)Cl]-catalyzed oxidation of para-substituted thioanisoles by PhI(OAc) $_2$  in CH $_3$ CN at  $23\pm 2$  °C. Labels show substituents on the para-position of substrates.

limiting amount of PhI(OAc) $_2$  (0.2 equiv.) was used in order to maintain similar concentrations of the paired substrates during the course of reactions. The amounts of oxidation products formed were determined by GC–MS analysis. Each sulfide substrate was oxidized to the corresponding sulfoxide with negligible sulfone (< 1%) from the overoxidation of the sulfoxide. Table 2 contains relative rate constants ratios ( $k_{\rm rel}$ ) from direct kinetic studies with 2 and 3, and product ratios from catalytic competition reactions. As evident in Table 2, the ratios of absolute rate constants of 2 found in direct kinetic studies differed

<sup>&</sup>lt;sup>b</sup> Ratios of absolute rate constants from kinetic results with chromium(IV)-oxo porphyrins (2).

 $<sup>^{\</sup>rm c}$  Ratios of absolute rate constants from kinetic results with chromium(V)-oxo porphyrins (3).



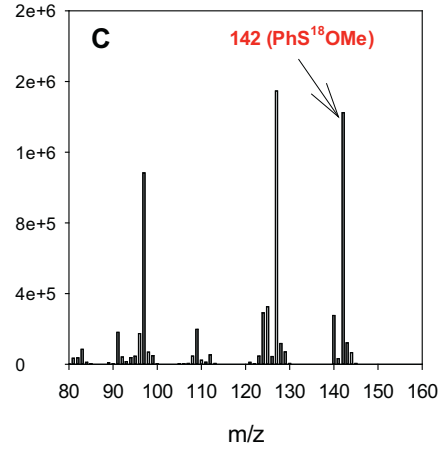


Fig. 8. (A) The representative GC traces for catalytic oxidation of thioanisole (0.5 mmol) with PhI(OAc)<sub>2</sub> by [Cr<sup>III</sup>(TPFPP)]Cl (1  $\mu$ mol) in CH<sub>3</sub>CN in the presence of H<sub>2</sub>O (10  $\mu$ L) over 12 h; (B) MS spectrum of sulfoxide product with H<sub>2</sub><sup>16</sup>O; (C) MS spectrum of sulfoxide product with H<sub>2</sub><sup>18</sup>O.

dramatically from the oxidation ratios for competition oxidation reactions of the two substrates in all systems studied here. In contrast, the ratio of rate constants for reactions of 3 with the paired substrates is similar to the ratio of products found in competitive catalytic oxidations (Table 2). Difference in inherent reactivities of the substrates obviously influence the ratio of products, but the close match between the ratios of absolute rate constants and the ratios of products from the competition experiment strongly suggests that chromium(V)-oxo 3 were the premier oxidants in the catalytic oxidation reactions,

Additional support for a Cr<sup>V</sup>-oxo oxidant involved in the catalytic oxidations is seen from the linear free-energy analysis for competitive oxidations of the para-substituted thioanisoles by catalyst 1a. Fig. 7 depicts a linear correlation (R=0.98) of  $\log k_{\rm rel}[k_{\rm rel}=k({\rm Y-thioanisole})/k$  (thioanisole)] versus Hammett  $\sigma^+$  substituent constant. The observed slope ( $\rho^+$ ) of the plot is – 1.71  $\pm$  0.22, almost identical to that observed in the direct kinetic studies of 3a with substituted thioanisoles ( $\rho^+=-1.69\pm0.17$ ). Importantly, when the catalytic sulfoxidation reaction by [Cr<sup>III</sup>(Por)Cl] with PhIO(Ac)<sub>2</sub> was carried out in the presence of a small amount of H<sub>2</sub><sup>8</sup>O (10  $\mu$ L), the corresponding <sup>18</sup>O-enriched sulfoxide product (m/z of 142) was detected by MS (Fig. 8). The competitive product studies, Hammett correlation analysis and the <sup>18</sup>O-isotope labelling experiment led us to conclude that the observed chromium(V)-oxo species is the primary oxidant under the catalytic turnover conditions, even though they could not be detected during the reactions.

#### 4. Conclusion

In conclusion, we report the generation and kinetic study of chromium(IV)-oxo and chromium(V)-oxo porphyrins in three systems for sulfide oxidation reactions. In addition to the chemical oxidation of chromium(III) complexes by PhI(OAc)2, the visible-light irradiation of chromium(III) chlorates provides alternative access to chromium(IV)oxo porphyrins. One-electron oxidation of [Cr<sup>IV</sup>(Por)(O)] by AgClO<sub>4</sub> produced chromium(V)-oxo species [Cr<sup>V</sup>(Por)(O)]<sup>+</sup> in CH<sub>3</sub>CN solution. The kinetic results from this work provide a direct comparison of reactivities of porphyrin-chromium(IV)/(V)-oxo complexes in sulfide oxidation reactions under identical conditions. As anticipated, chromium(V)-oxo species are orders of magnitude more reactive than the corresponding chromium(IV)-oxo porphyrins, in which the substantially greater rate constants were obtained with electron-deficient [Cr<sup>V</sup>(TDFPP)(O)]<sup>+</sup> and [Cr<sup>V</sup>(TPFPP)(O)]<sup>+</sup> systems than those with the electron-rich [Cr<sup>V</sup>(TMP)(O)]<sup>+</sup>. The order of reactivity of [Cr<sup>IV</sup>(Por)(O)] and  $[Cr^{V}(Por)(O)]^{+}$  for the oxidation of the same substrate follows TPFPP > TDFPP > TMP, consistent with the expectation for electrophilic metal-oxo oxidants based on the electron-demand of the ligands.

Hammett analyses with conventional  $\sigma^+$  values gave a linear correlation in reactions of substituted thioanisoles with  $[Cr^V(Por)(O)]^+$ , indicating a positive charge developed on the benzylic sulfur atom during the transition states. The kinetic, spectral and Hammett correlation studies suggest that sulfoxidation reaction with  $[Cr^V(Por)(O)]^+$  most likely proceeds through the electrophilic attack mechanism with the formation of a sulfur cation in the rate-determining step. In addition, the competition product studies implicated that the chromium(V)-oxo species observed in the kinetic studies is the primary oxidant for the catalytic sulfide oxidations by chromium(III) porphyrins with PhI(OAc)<sub>2</sub>.

## CRediT authorship contribution statement

**Tristan Skipworth:** Investigation, Validation, Visualization. **Mardan Khashimov:** Investigation, Visualization. **Iyanu Ojo:** Investigation, Visualization. **Rui Zhang:** Conceptualization, Methodology, Writing – original draft, Supervision, Funding acquisition.

# **Declaration of Competing Interest**

The authors declare that they have no known competing financial interests or personal relationships that could have appeared to influence the work reported in this paper.

## Data availability

Data will be made available on request.

### Acknowledgment

We greatly appreciate the National Science Foundation (CHE 1764315 and CHE 2154579) for supporting this research. Instrumentation of this work was also supported in part by a grant from the National Science Foundation (MRI 1919501). T. Skipworth and I. Ojo are thankful to the WKU Office of Research for awarding internal grants. We thank Mr. Seth Klaine for his assistance on the photochemical generation of chromium(IV)-oxo species. We also thank Ms. Pauline Norris of the Advanced Material Institute at WKU for assistance with ESI-MS measurements.

#### Appendix A. Supplementary data

Supplementary data to this article can be found online at https://doi.org/10.1016/j.jinorgbio.2022.112006.

#### References

- [1] C. He, J. Cheng, X. Zhang, M. Douthwaite, S. Pattisson, Z. Hao, Recent advances in the catalytic oxidation of volatile organic Compounds: a review based on pollutant sorts and sources, Chem. Rev. 119 (2019) 4471–4568.
- [2] X. Huang, J.T. Groves, Oxygen activation and radical transformations in Heme proteins and Metalloporphyrins, Chem. Rev. 118 (2018) 2491–2553.
- [3] J.E. Baeckvall, Modern Oxidation Methods, Wiley-VCH Verlag, Weinheim, 2011.
- [4] T. Punniyamurthy, S. Velusamy, J. Iqbal, Recent advances in transition metal catalyzed oxidation of organic substrates with molecular oxygen, Chem. Rev. 105 (2005) 2329–2363.
- [5] P.R. Ortiz de Montellano, Cytochrome P450 Structure, Mechanism, and Biochemistry, Cytochrome P450 Structure, Mechanism, and Biochemistry, Kluwer Academic/Plenum, New York, 2005.
- [6] I.G. Denisov, T.M. Makris, S.G. Sligar, I. Schlichting, Structure and chemistry of cytochrome P 450, Chem. Rev. 105 (2005) 2253–2277.
- [7] B. Meunier, Metalloporphyrins as versatile catalysts for oxidation reactions and oxidative DNA cleavage, Chem. Rev. 92 (1992) 1411–1456.
- [8] R.A. Sheldon, Metalloprophyrins In Catalytic Oxidations, Marcel Dekker, New York 1904
- [9] C.-M. Che, J.-S. Huang, Metalloporphyrin-based oxidation systems: from bioimetic reactions to application in organic synthesis, Chem. Commun. 3996-4015 (2009).
- [10] H.-Y. Liu, M.H.R. Mahmood, S.-X. Qiuc, C.K. Chang, Recent developments in manganese corrole chemistry, Coord. Chem. Rev. 257 (2013) 1306–1333.
- [11] C.J. Pereira Monteiro, M.A. Ferreira Faustino, M.D.G. Pinho Morgado Silva Neves, M.M. Quialheiro Simões, E. Sanjust, Metallophthalocyanines as catalysts in aerobic oxidation, Catalysts 11 (2021) 122.
- [12] B. Meunier, Metal-Oxo and Metal-Peroxo Species in Catalytic Oxidations, Springer-Verlag, Berlin, 2000.
- [13] M. Costas, M.P. Mehn, M.P. Jensen, L. Que, Dioxygen activation at mononuclear nonheme iron active sites: enzymes, models, and intermediates, Chem. Rev. 104 (2004) 939–986
- [14] H. Fujii, Electronic structure and reactivity of high-valent oxo iron porphyrins, Coord. Chem. Rev. 226 (2002) 51–60.
- [15] D.P. Goldberg, Corrolazines: new Frontiers in high-valent metalloporphyrinoid stability and reactivity, Acc. Chem. Res. 40 (2007) 626–634.
- [16] H.M. Neu, R.A. Baglia, D.P. Goldberg, A balancing act: stability versus reactivity of Mn(O) complexes, Acc. Chem. Res. 48 (2015) 2754–2764.
- [17] R.A. Baglia, J.P.T. Zaragoza, D.P. Goldberg, Biomimetic reactivity of oxygenderived manganese and iron porphyrinoid complexes, Chem. Rev. 117 (2017) 13320–13352.
- [18] J. Rittle, M.T. Green, Cytochrome P450 compound I: capture, characterization, and C-H bond activation kinetics, Science 330 (2010) 933–937.
- [19] T.C. Poulos, Heme enzyme structure and function, Chem. Rev. 114 (2014) 3919–3962.
- [20] R. Zhang, S. Klaine, C. Alcantar, F. Bratcher, Visible light generation of high-valent metal-oxo intermediates and mechanistic insights into catalytic oxidations, J. Inorg. Biochem. 212 (2020), 111246.
- [21] K.W. Kwong, C.M. Winchester, R. Zhang, Photochemical generation of manganese (IV)-oxo porphyrins by visible light photolysis of dimanganese(III) l-oxo bisporphyrins, Inorg. Chim. Acta 451 (2016) 202–206.
- [22] S. Klaine, F. Bratcher, C.M. Winchester, R. Zhang, Formation and kinetic studies of manganese(IV)-oxo porphyrins: oxygen atom transfer mechanism of sulfide oxidations, J. Inorg. Biochem. 204 (2020), 110986.
- [23] T.H. Chen, N. Asiri, K.W. Kwong, J. Malone, R. Zhang, Ligand control in the photochemical generation of high-valent porphyrin-iron-oxo derivatives, Chem. Commun. 51 (2015) 9949–9952.
- [24] K.W. Kwong, D. Patel, J. Malone, N.F. Lee, B. Kash, R. Zhang, An investigation of ligand effects on the visible light-induced formation of porphyrin-iron(IV)-oxo intermediates, New J. Chem. 41 (2017) 14334–14341.
- [25] Y. Huang, E. Vanover, R. Zhang, A facile photosynthesis of trans-dioxoruthenium (VI) porphyrins, Chem. Commun. 46 (2010) 3776–3778.
- [26] R. Zhang, Y. Huang, C. Abebrese, H. Thompson, E. Vanover, C. Webb, Generation of trans-dioxoruthenium(VI) porphyrins: a photochemical approach, Inorg. Chim. Acta 372 (2011) 152–157.
- [27] K.W. Kwong, N.F. Lee, D. Ranburg, J. Malone, R. Zhang, Visible light-induced formation of corrole-manganese(V)-oxo complexes: observation of multiple oxidation pathways, J. Inorg. Biochem. 163 (2016) 39–44.
- [28] N.F. Lee, J. Malone, H. Jeddi, K.W. Kwong, R. Zhang, Visible-light photolysis of corrole-manganese(IV) nitrites to generate corrole-manganese(V)-oxo complexes, Inorg. Chem. Commun. 82 (2017) 27–30.
- [29] S. Klaine, N.F. Lee, A. Dames, R. Zhang, Visible light generation of chromium(V)-oxo salen complexes and mechanistic insights into catalytic sulfide oxidation, Inorg. Chim. Acta 509 (2020), 119681.
- [30] D.N. Harischandra, R. Zhang, M. Newcomb, Photochemical generation of a highly reactive Iron-Oxo intermediate. A true Iron(V)-Oxo species? J. Am. Chem. Soc. 127 (2005) 13776–13777.
- [31] D.N. Harischandra, G. Lowery, R. Zhang, M. Newcomb, Production of a putative Iron(V)—Oxo corrole species by photo-disproportionation of a Bis-Corrole—Diiron (IV)—μ-Oxo dimer: implication for a green oxidation catalyst, Org. Lett. 11 (2009) 2009 2002
- [32] R. Zhang, E. Vanover, T.-H. Chen, H. Thompson, Visible light-driven aerobic oxidation catalyzed by a diiron(IV)  $\mu$ -oxo biscorrole complex, Appl. Catal. A 465 (2013) 95–100.

- [33] R. Zhang, E. Vanover, W.-L. Luo, M. Newcomb, Photochemical generation and kinetic studies of a putative porphyrin-ruthenium(V)-oxo species, Dalton Trans. 43 (2014) 8749–8756.
- [34] E. Vanover, Y. Huang, L. Xu, M. Newcomb, R. Zhang, Photocatalytic aerobic oxidation by a bis-porphyrin-ruthenium(VI) μ-Oxo dimer: observation of a putative porphyrin-ruthenium(V)-Oxo intermediate, Org. Lett. 12 (2010) 2246–2249.
- [35] R. Zhang, J.H. Horner, M. Newcomb, Laser flash photolysis generation and kinetic studies of porphyrin-manganese-Oxo intermediates. Rate constants for oxidations effected by porphyrin-MnV-Oxo species and apparent disproportionation equilibrium constants for porphyrin-MnIV-Oxo species, J. Am. Chem. Soc. 127 (2005) 6573–6582.
- [36] R. Zhang, M. Newcomb, Laser flash photolysis generation of high-valent transition metal-Oxo species: insights from kinetic studies in real time, Acc. Chem. Res. 41 (2008) 468–477.
- [37] J.T. Groves, W.J. Kruper, Metalloporphyrins in oxidative catalysis. Oxygen transfer reactions of oxochromium porphyrins, Israel J. Chem. 25 (1985) 148–154.
- [38] J. Muzart, Chromium-catalyzed oxidations in organic synthesis, Chem. Rev. 92 (1992) 113–140.
- [39] J.T. Groves, W.J. Kruper, Preparation and characterization of an Oxoporphinatochromium(V) complex, J. Am. Chem. Soc. 101 (1979) 7613–7615.
- [40] J.T. Groves, R.C. Haushalter, E.S.R., Evidence for chromium(v) porphyrinates, Chem. Commun. (1981) 1165–1166.
- [41] S.E. Creager, R. Murray, Electrochemical studies of Oxo(meso-tetraphenylporphinato)chromium(IV). Direct evidence for epoxidation of olefins by an electrochemically generated formal chromium(V) state, Inorg. Chem. 24 (1985) 3824–3828.
- [42] H. Fujii, T. Yoshimura, H. Kamada, ESR studies of Oxochromium(V) porphyrin complexes: electronic structure of the CrV=O moiety, Inorg. Chem. 36 (1997) 1122–1127.
- [43] M.J. Garrison, T.C. Bruice, Intermediates in the epoxidation of alkenes by cytochrome P-450 models. 3. Mechanism of oxygen transfer from substituted Oxochromium(V) porphyrins to Olefinic substrates, J. Am. Chem. Soc. 111 (1989) 191–198
- [44] M.J. Garrison, D. Ostovic, T.C. Bruice, Is a linear relationship between the free energies of activation and one-Electron oxidation potential evidence for one-Electron transfer being rate determining? Intermediates in the epoxidation of alkenes by cytochrome P-450 models. 4. Epoxidation of a series of alkenes by Oxo (mejotetrakis(2,6-dibromophenyl)porphinato)-chromium(V), J. Am. Chem. Soc. 111 (1989) 4901–4966.
- [45] D. Ostovic, T.C. Bruice, Mechanism of alkene epoxidation by iron, chromium, and manganese higher valent oxo-metalloporphyrins, Acc. Chem. Res. 25 (1992) 314–320.
- [46] J. Lindsey, R.D. Wagner, Investigation of the synthesis of ortho-substituted tetraphenylporphyrins, J. Organomet. Chem. 54 (1989) 828–836.
- [47] A.D. Adler, F.R. Longo, F. Kampas, J. Kim, On the preparation of metalloporphyrins, J. Inorg. Nucl. Chem. 32 (1970) 2443–2445.
- [48] J.T. Groves, W.J. Kruper, R.C. Haushalter, W.M. Butler, Synthesis, characterization, and molecular structure of Oxo (porphyrinato) chromium (IV) complexes, Inorg. Chem. 21 (1982) 1363–1368.
- [49] N.-F. Lee, D. Patel, H.Y. Liu, R. Zhang, Insights from kinetic studies of photogenerated compound II models: reactivity toward aryl sulfides, J. Inorg. Biochem. 183 (2018) 56–65.
- [50] D. Dolphin, T.G. Traylor, L.Y. Xie, Polyhaloporphyrins: unusual ligands for metals and metal-catalyzed oxidations, Acc. Chem. Res. 30 (1997) 251–259.
- [51] H. Fujii, Effects of the electron-withdrawing power of substituents on the electronic structure and reactivity in oxoiron(IV) porphyrin .pi.-cation radical complexes, J. Am. Chem. Soc. 115 (1993) 4641–4648.
- [52] D. Liston, B.O. West, Oxochromium compounds. 2. Reaction of oxygen with chromium(II) and chromium(III) porphyrins and synthesis of a μ- chromium porphyrin derivative, Inorg. Chem. 24 (1985) 1568–1576.
- [53] J.H. In, S.E. Park, R. Song, W. Nam, Iodobenzene diacetate as an efficient terminal oxidant in iron(III) porphyrin complex-catalyzed oxygenation reactions, Inorg. Chim. Acta 343 (2003) 373–376.
- [54] D. Ranburger, B. Willis, B. Kash, H. Jeddi, C. Alcantar, R. Zhang, Synthetic and mechanistic investigations on manganese corrole-catalyzed oxidation of sulfides with iodobenzene diacetate, Inorg. Chim. Acta 487 (2019) 41–49.
- [55] M. Yamaj, Y. Hama, Y. Miyazaki, M. Hoshino, Photochemical formation of oxochromium(IV) tetraphenylporphyrin from nitritochromium(HI) tetraphenylporphyrin in benzene, Inorg. Chem. 31 (1992) 932–934.
- [56] R.J. Radford, M.D. Lim, R.S. Da Silva, P.C. Ford, Photochemical cleavage of nitrate ion coordinated to a Cr(III) porphyrin, J. Coord. Chem. 63 (2010) 2743–2749.
- [57] Z. Pan, M. Newcomb, Kinetics and mechanism of oxidation reactions of porphyriniron(IV)-oxo intermediates, Inorg. Chem. 46 (2007) 6767–6774.
- [58] J.T. Groves, Z. Gross, M.K. Stern, Preparation and reactivity of Oxoiron(IV) porphyrins, Inorg. Chem. 33 (1994) 5065–5072.
- [59] F.P. Guengerich, T.L. MacDonald, Chemical mechanisms of catalysisby cytochromes P-450: a unified view, Acc. Chem. Res. 17 (1984) 9–16.
- [60] R. Zhang, W.-Y. Yu, H.-Z. Sun, W.-S. Liu, C.-M. Che, Stereo- and enantioselective alkene epoxidations: a comparative study of D4- and D2-symmetric homochiral trans-dioxoruthenium(VI) porphyrins, Chem. Eur. J. 8 (2002) 2495–2507.
- [61] C.-M. Che, J.-L. Zhang, R. Zhang, J.-S. Huang, T.-S. Lai, W.-M. Tsui, X.-G. Zhou, Z.-Y. Zhou, N. Zhu, C.K. Chang, Hydrocarbon oxidation by beta-halogenated dioxoruthenium(VI) porphyrin complexes: effect of reduction potential (RuVI/V) and C-H bond-dissociation energy on rate constants, Chem. Eur. J. 11 (2005) 7040–7053.

- [62] C. Abebrese, Y. Huang, A. Pan, Z. Yuan, R. Zhang, Kinetic studies of oxygen atom transfer reactions from trans-dioxoruthenium(VI) porphyrins to sulfides, J. Inorg. Biochem. 105 (2011) 1555–1561.
- [63] J.H. Aquaye, J.C. Muller, K.J. Takeuchi, Oxidation of thioanisoles and methyl phenyl sulfoxides by Oxo(phosphine)ruthenium(IV) complexes, Inorg. Chem. 32 (1993) 160–165.
- [64] A. Chellamani, S. Harikengaram, J. Phys. Org. Chem. 16 (2003) 589-597.
- [65] R. Sevvel, S. Rajagopal, C. Srinivasan, N. Ismail Alhaji, A. Chellamani, Mechanism of selective oxidation of organic sulfides with Oxo(salen)chromium(V) complexes, J. Organomet. Chem. 65 (2000) 3334–3340.
- [66] A. Chellamani, P. Kulanthaipandi, S. Rajagopal, Oxidation of aryl methyl sulfoxides by Oxo(salen)manganese(V) complexes and the reactivity–selectivity principle, J. Organomet. Chem. 64 (1999) 2232–2239.
- [67] A. Kumar, I. Goldberg, M. Botoshansky, Y. Buchman, Z. Gross, Oxygen atom transfer reactions from isolated (Oxo)manganese(V) Corroles to sulfides, J. Am. Chem. Soc. 132 (2010) 15233–15245.

- [68] R. Zhang, N. Nagraj, D.S.P. Lansakara-P, L.P. Hager, M. Newcomb, Kinetics of two-Electron oxidations by the compound I derivative of chloroperoxidase, a model for cytochrome P450 oxidants, Org. Lett. 8 (2006) 2731–2734.
- [69] T.G. Traylor, T. Nakano, B.E. Dunlap, P.S. Traylor, D. Dolphin, Mechanisms of hemin-catalyzed alkene epoxidation. The effect of catalyst on the regiochemistry of epoxidation, J. Am. Chem. Soc. 108 (1986) 2782–2784.
- [70] A.J. Castellino, T.C. Bruice, Intermediates in the epoxidation of alkenes by cytochrome P-450 models. cis-Stilbene as a mechanistic probe, J. Am. Chem. Soc. 110 (1988) 158–162.
- [71] W.M. Schubert, J.R. Keefe, The acid-catalyzed hydration of styrenes, J. Am. Chem. Soc. 94 (1972) 559–566.
- [72] K. Yates, R.S. McDonald, S.A. Shapiro, Kinetics and mechanisms of electrophilic addition. I. Comparison of second- and third- order brominations, J. Organomet. Chem. 38 (1973) 2460–2464.